

Theoretical Study of Hydroxide Ion–Water Clusters

Sotiris S. Xantheas

Contribution from the Theory, Modeling and Simulation, Environmental Molecular Sciences Laboratory, Pacific Northwest Laboratory, P.O. Box 999, MS K1-83, Richland, Washington, 99352

Received May 3, 1995[®]

Abstract: The optimal structures, harmonic vibrational frequencies, and incremental association enthalpies for the $\text{OH}^-(\text{H}_2\text{O})_n$ ($n = 1-3$) clusters have been computed at the MP2/aug-cc-p VDZ level of theory, the first ones reported at the correlated level for the $n = 2$ and 3 clusters. The incremental association enthalpies at 298 K were estimated at -27.0 , -20.1 , and -16.9 kcal/mol, respectively, within the error bars of recent experimental measurements for the $n = 1, 2$, and 3 clusters. Two almost isoenergetic isomers were identified for the $n = 3$ cluster. Hydrogen bonding between water molecules was found in the $n = 3$ but not the $n = 2$ cluster, the structure of which is determined by the strong hydroxide ion–water interaction. Hydration of the hydroxide ion results in a decrease in its bond length with an accompanying increase in the analogous frequency that eventually “scrambles” with the one of the “free” (non-hydrogen bonded) stretches in water. The most active infrared (IR) modes correspond to OH stretches which are hydrogen bonded to the hydroxide ion in the range $2500-3000\text{ cm}^{-1}$ in agreement with experimental infrared multiple internal reflectance (IR-MIR) measurements of aqueous hydroxide.

I. Introduction

The importance of molecular clusters has been recently recognized¹ because of their role in understanding the transition from gas to condensed phase environments. Aqueous clusters of the hydroxide ion are of particular significance because of their involvement in cluster and condensed phase acid–base chemistry. Information regarding the hydration of OH^- can be extracted from IR and Raman studies² of aqueous alkali metal hydroxides. The results of these experiments suggest that OH^- is a poor hydrogen bond donor but an excellent hydrogen bond acceptor. The position of the OH^- vibration in the IR spectra³ and the difference in intensities in the Raman spectra⁴ for the OH^- symmetric stretching mode support the proposition that the OH group is not strongly hydrogen bonded through the hydrogen but there exists a strong hydrogen bond from the hydroxide oxygen to a water hydrogen. On the basis of the variation of the absorption with hydroxide concentration during infrared multiple internal reflectance (MIR) measurements,³ it was proposed that one water molecule adds to the OH^- group to form H_3O_2^- and at least two additional water molecules may hydrate this species. It is readily seen that understanding the properties of $\text{OH}^-(\text{H}_2\text{O})_n$ clusters represents a useful complement to the solution data²⁻⁴ toward the goal of elucidating the effect of hydration on OH^- .

Aqueous clusters of the hydroxide ion have been previously studied both experimentally⁵⁻¹² and theoretically.¹³⁻²⁰ During

experiments studying the dissociative attachment of electrons to water vapor, Klots and Compton⁵ observed clusters with 3 waters and Knapp *et al.*⁶ reported clusters with up to 30 waters. Yang and Castleman⁸ used a flow tube reactor to produce larger clusters with as many as 60 waters. They found that hydroxide ion clusters with 11, 14, 17, and 20 water molecules have increased stability as indicated by the existence of anomalous discontinuities (often referred to as “magic numbers”) in the intensity of the mass spectra. Small hydroxide ion–water clusters were studied by van Doren *et al.*⁷ using a tandem flowing afterglow selected ion flow tube drift apparatus. They observed that $\text{OH}^-(\text{H}_2\text{O})$ was generated almost exclusively from $\text{OH}^-(\text{H}_2\text{O})_3$ following collisional dissociation in the reaction flow tube. By measuring the thresholds for collision-induced dissociation reactions of hydrated OD^- ions, De Paz *et al.*⁹ determined incremental heats of hydration of -34.6 , -23.1 , and -18.4 kcal/mol for the successive addition of the first three water molecules to OD^- . Ashadi and Kebarle¹⁰ used a high-pressure ion source that utilizes 2000 eV electrons for the ionization to study clustering equilibria and determined incremental enthalpies of hydration of -22.5 , -16.4 , -15.1 , -14.2 , and -14.1 kcal/mol for the successive addition of up to 5 water molecules to OH^- . These experiments determined incremental enthalpies that were substantially lower than the (non equilibrium) ones of De Paz *et al.*,⁹ but they were done with the continuous ionization method and therefore did not follow the

[®] Abstract published in *Advance ACS Abstracts*, September 15, 1995.
 (1) Clusters: A new state of matter. *LBL Res. Rev.* **1991**, 16, 2.
 (2) Giguère, P. A. *Rev. Chim. Miner.* **1983**, 20, 588.
 (3) Maiorov, V. D.; Bocharova, L. V.; Librovich, N. B. *Russ. J. Phys. Chem.* **1982**, 56, 67. Librovich, N. B.; Maiorov, V. D. *Russ. J. Phys. Chem.* **1982**, 56, 380. Maiorov, V. D.; Librovich, N. B.; Bikbaeva, G. G.; Vinnik, M. I. *Russ. J. Phys. Chem.* **1978**, 52, 688.
 (4) Busing, W. R.; Hornig, D. F. *J. Phys. Chem.* **1961**, 65, 284.
 (5) Klots, C. E.; Compton, R. N. *J. Chem. Phys.* **1978**, 69, 1644.
 (6) Knapp, M.; Echt, O.; Kreisler, D.; Recknagel, E. *J. Chem. Phys.* **1986**, 85, 636.
 (7) van Doren, J. M.; Barlow, S. E.; Depuy, C. H.; Bierbaum, V. M. *Int. J. Mass Spectrom. Ion Proc.* **1987**, 81, 85.
 (8) Yang, X.; Castleman, A. W., Jr. *J. Phys. Chem.* **1990**, 94, 8500.
 (9) De Paz, M.; Giardini, A. G.; Friedman, L. *J. Chem. Phys.* **1970**, 52, 687.

(10) Ashadi, M.; Kebarle, P. *J. Phys. Chem.* **1970**, 74, 1483.
 (11) Payzant, J. D.; Yamdagni, R.; Kebarle, P. *Can. J. Chem.* **1971**, 49, 3308.
 (12) Meot-Ner (Mautner), M.; Speller, C. V. *J. Phys. Chem.* **1986**, 90, 6616.
 (13) Newton, M. D.; Ehrenson, S. *J. Am. Chem. Soc.* **1971**, 93, 4971.
 (14) Szczesniak, M. M.; Scheiner, S. *J. Chem. Phys.* **1982**, 77, 4586.
 (15) McMichael Rohlffing, C.; Allen, L. C.; Cook, C. M. *J. Chem. Phys.* **1983**, 78, 2498.
 (16) Sapsee, A.-M.; Osorio, L.; Snyder, G. *Int. J. Quantum Chem.* **1984**, 26, 223.
 (17) Ohta, K.; Morokuma, K. *J. Phys. Chem.* **1985**, 89, 5845.
 (18) Andrés, J. L.; Durán, M.; Lledós, A.; Bertrán, J. *Chem. Phys. Lett.* **1986**, 124, 177.
 (19) Carbonell, E.; Andrés, J. L.; Lledós, A.; Durán, M.; Bertrán, J. *J. Am. Chem. Soc.* **1988**, 110, 996.
 (20) De Bene, J. E. *J. Phys. Chem.* **1988**, 92, 2874.

time dependence of the ion concentrations. In order to place the equilibrium data on a firmer footing, Payzant, Yamdagni, and Kebarle¹¹ repeated the equilibrium experiments using a pulsed electron beam and determined incremental enthalpies of formation of -25.0 and -17.9 kcal/mol for the $n = 1, 2$ clusters, respectively, slightly higher than their initial estimates¹⁰ but still substantially lower than the ones determined during non-equilibrium studies.⁹ A more recent measurement by Meot-Ner (Mautner) and Speller¹² using a pulsed high-pressure mass spectrometer produced incremental enthalpies of -26.5 , -17.6 , -16.2 , -12.0 , -11.5 , -11.2 , and -10.4 kcal/mol for the successive addition of up to 7 water molecules to OH^- . The last set of results confirmed the range of Kebarle's estimates^{10,11} and at the same time suggested a shell effect after $n = 3$.

The initial discrepancy in the experimentally estimated enthalpy of formation for the $n = 1$ cluster (-22.5 to -34.6 kcal/mol) has fueled several theoretical studies¹³⁻²⁰ aimed at the computation of its optimal structure and binding energy. The minimum energy geometry of the $n = 1$ cluster corresponds to the chain structure $[\text{HO}\cdots\text{H}\cdots\text{OH}]^-$. The potential energy surface (PES) for the proton transfer between the two oxygen atoms corresponds to a double well potential characterized by a low barrier. Newton and Ehrenson¹³ reported a binding energy of -40.7 kcal/mol for the $n = 1$ cluster at the Hartree-Fock (HF) level of theory with the 4-31G basis set. They also performed HF calculations for the $n = 2$ and 3 clusters at symmetry constrained geometries. Szczesniak and Scheiner¹⁴ reported binding energies of -34.2 , -42.7 , and -40.4 kcal/mol for the $n = 1$ cluster at the HF, second- and third-order perturbation theory (MP2, MP3) levels with the 6-311G** basis set. However, by augmenting the 6-311G** basis set with a set of very diffuse p functions on oxygen, they obtained binding energies of -23.9 and -27.1 kcal/mol at the HF and MP3 levels of theory, respectively. They found that electron correlation resulted in a flattening of the PES such that the barrier to proton transfer is considerably below the lowest vibrational level for protonic motion. A similar study by Rohlffing, Allen, Cook, and Schlegel¹⁵ with the 6-31G** basis set failed to locate a stable asymmetric structure at the MP2 level of theory. Sapse, Osorio, and Synder¹⁶ reported incremental binding energies of -38.9 , -29.4 , -24.3 , and -1.9 kcal/mol for the $n = 1-4$ clusters at the HF/6-31G level of theory which are, however, in large discrepancy with the experimentally determined ones.^{11,12} Incremental energies of -25.3 and -23.2 kcal/mol were reported by Ohta and Morokuma¹⁷ for the $n = 1$ and 2 clusters at the HF level with the 6-31G* basis set augmented with a set of p functions on both the oxygen and hydrogen atoms. Again, the incremental binding energy for the $n = 2$ cluster is too high with respect to the experimental value¹² of -17.6 kcal/mol. Hartree-Fock calculations with the 4-31G basis set addressing the correlation between proton transfer and solvent motion¹⁸ as well as the charge transfer¹⁹ in H_3O_2^- have also appeared in the literature. Finally, Del Bene reported²⁰ an enthalpy of -26.4 kcal/mol for the $n = 1$ cluster at the MP4/6-31+G(2d,2p) level of theory.

To date, *ab initio* calculations that include electron correlation have been reported only for the $n = 1$ cluster. In this study we present *ab initio* correlated calculations for the hydroxide ion clusters with as many as 3 water molecules. In Section II we outline the computational details of our calculations. The results for the optimal structures, vibrational spectra, and energetics of the $n = 1-3$ clusters together with the discussion of the trends with cluster size will be reported in Sections IIIa-c. Final conclusions were presented in Section IV.

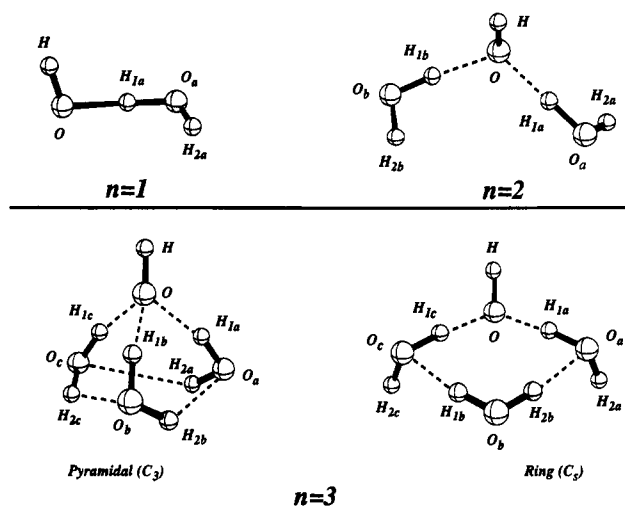


Figure 1. Optimal structures of the $\text{OH}^-(\text{H}_2\text{O})_n$ ($n = 1-3$) clusters with labeling of the atoms.

II. Computational Details

The survey of previous theoretical work on hydroxide ion-water clusters suggests that both electron correlation and basis sets encompassing diffuse functions are needed in order to produce accurate energetics and describe the subtle features of the $n = 1$ potential energy surface corresponding to proton transfer. We have optimized the geometries of the $n = 1-3$ clusters at the second-order perturbation theory (MP2) level of theory with the augmented correlation-consistent polarized valence set²¹ of double- ζ (aug-cc-pVDZ) quality. The aug-cc-pVDZ set for oxygen consists of a (9s4p1d) primitive set contracted to [3s2p1d] and augmented with an extra set of diffuse (spd) primitive functions optimized for the oxygen negative ion. For hydrogen, the aug-cc-pVDZ set is (4s1p) contracted to [2s1p] and augmented with a diffuse (sp) set of primitive functions, again optimized for the negative ion (H^-). This level of theory was chosen as a compromise between feasibility and accuracy in earlier benchmark studies of water²²⁻²⁴ and negative ion-water^{25,26} clusters. The geometry of the $n = 1$ cluster was also optimized with the larger aug-cc-pVTZ set at the MP2 level in order to investigate the effect of the basis set on the optimal geometry. For d and f sets of basis functions we retained only the 5 with true d and 7 with true f character, respectively. The total number of basis functions is 32 and 69 for OH and 41 and 92 per water molecule for the augmented double- and triple- ζ sets, respectively. During the MP2 calculations all electrons were correlated. All harmonic vibrational frequencies were computed analytically. Enthalpies of formation at 298 K were estimated using the scheme proposed by Pople and co-workers.²⁷ All calculations were performed with the Gaussian-92 suite of programs.²⁸ During all geometry optimizations the "very tight" criterion was used (the largest component of the gradient was converged to a value less than 2×10^{-6} au).

III. Results and Discussion

a. Optimal Structures. The optimal structures of the $n = 1-3$ clusters with the labeling of the atoms are shown in Figure 1. Their internal coordinates, together with those for OH^- and

(21) Dunning, T. H., Jr. *J. Chem. Phys.* **1989**, *90*, 1007. Kendall, R. A.; Dunning, T. H., Jr.; Harrison, R. J. *J. Chem. Phys.* **1992**, *96*, 6796.

(22) Xantheas, S. S.; Dunning, T. H., Jr. *J. Chem. Phys.* **1993**, *98*, 8037.

(23) Xantheas, S. S.; Dunning, T. H., Jr. *J. Chem. Phys.* **1993**, *99*, 8774.

(24) Xantheas, S. S. *J. Chem. Phys.* **1994**, *100*, 7523.

(25) Xantheas, S. S.; Dunning, T. H., Jr. *J. Phys. Chem.* **1992**, *96*, 7505.

(26) Xantheas, S. S.; Dunning, T. H., Jr. *J. Phys. Chem.* **1994**, *98*, 13489.

(27) Del Bene, J. E.; Mettee, H. D.; Frisch, M. J.; Luke, B. T.; Pople, J. A. *J. Chem. Phys.* **1983**, *87*, 3279.

(28) GAUSSIAN 92, Revision C; M. J. Frisch, G. W. Trucks, M. Head-Gordon, P. M. W. Gill, M. W. Wong, J. B. Foresman, B. G. Johnson, H. B. Schlegel, M. A. Robb, E. S. Replogle, R. Gomperts, J. L. Andres, K. Raghavachari, J. S. Binkley, C. Gonzalez, R. L. Martin, D. J. Fox, D. J. Defrees, J. Baker, J. J. P. Stewart, and J. A. Pople; Gaussian, Inc.: Pittsburgh, PA, 1992.

Table 1. Optimal Internal Coordinates of OH⁻, H₂O, and OH⁻(H₂O)_{*n*} (*n* = 1–3) at the MP2/aug-cc-pVDZ Level of Theory^a

internal coordinate	OH ⁻	H ₂ O	OH ⁻ (H ₂ O)	OH ⁻ (H ₂ O) ₂	OH ⁻ (H ₂ O) ₃	
					pyramidal	ring
<i>R</i> (O–H), Å	0.973 (0.964)		0.969 (0.961)	0.967	0.964	0.966
<i>R</i> (O _a –H _{1a}), Å		0.965 (0.959)	1.089 (1.107)	1.038	1.008	1.044
<i>R</i> (O _a –H _{2a}), Å		0.965 (0.959)	0.965 (0.959)	0.965	0.967	0.966
φ(H _{2a} –O _a –H _{1a}), deg		103.8 (104.3)	101.4 (102.0)	101.7	99.7	102.3
<i>R</i> (O–H _{1a}), Å			1.426 (1.364)	1.543	1.656	1.513
α(O–H _{1a} –O _a), deg			177.0 (177.9)	176.0	162.9	174.2
α(H–O–H _{1a}), deg			106.1 (105.0)	108.5	127.0	111.3
δ[O–(H _{1a} –O _a –H _{2a})], deg			337.4 (334.0)	15.4	33.4	61.0
δ[H–(O–O _a –H _{2a})], deg			100.8 (101.3)	241.9	228.1	230.2
α(O _a –O–O _b), deg				115.6	78.1	51.5
<i>R</i> (O _b –H _{1b}), Å				1.033		0.979
<i>R</i> (O _b –H _{2b}), Å				0.965		0.979
φ(H _{2b} –O _b –H _{1b}), deg				101.5		101.4
<i>R</i> (O–H _{1b}), Å				1.559		3.175
α(O–H _{1b} –O _b), deg				176.0		115.5
α(H–O–H _{1b}), deg				109.0		128.2
δ[O–(H _{1b} –O _b –H _{2b})], deg				15.3		2.8
δ[H–(O–O _b –H _{2b})], deg				250.8		271.8
<i>R</i> (O _a –O _b), Å				4.375	3.321	2.907

^a Numbers in parentheses denote values with the aug-cc-pVTZ set. The definition of the atoms is given in Figure 1.

H₂O, are listed in Table 1; numbers in parentheses correspond to the MP2 results with the aug-cc-pVTZ set. In agreement with previous studies, we find that the water molecule binds to the oxygen atom of the hydroxide ion via an almost linear hydrogen bond. The fact that this hydrogen bond is very strong results in a large distortion of the water molecule, similar to the one observed for the F⁻(H₂O) cluster²⁶ for which the hydrogen bond strength is of comparable magnitude. The hydrogen bonded *R*(O_a–H_{1a}) bond distance is 1.089 Å, the “free” *R*(O_a–H_{2a}) bond length remains unchanged with respect to water, and the (H–O–H) angle is 101.4°. The nuclear arrangement at the equilibrium geometry readily allows for isomerization via transfer of H_{1a} between the two oxygen atoms O and O_a (cf. Figure 1). The electronic energy barrier for this isomerization is very small (0.3 kcal/mol at the MP2/aug-cc-pVDZ level of theory). Inclusion of zero-point vibrational energy corrections stabilizes the symmetric transition state more than the asymmetric minima, therefore resulting in a barrierless motion of the hydrogen bonded proton between the two oxygen atoms. Furthermore, the difference between *R*(O_a–H_{1a}) and *R*(O–H_{1a}) decreases from 0.337 Å to 0.257 Å with the larger aug-cc-pVTZ basis set, suggesting an even more lower electronic energy barrier with the larger basis set. The relative changes in the other intramolecular internal coordinates of the *n* = 1 cluster with the larger aug-cc-pVTZ set are comparable to the corresponding ones in water. An extensive study of the *n* = 1 PES will be presented elsewhere.

The optimal geometry of the *n* = 2 cluster is qualitatively similar to the one reported earlier for the F⁻(H₂O)₂ and H⁻(H₂O)₂ clusters.^{25,26} The two water molecules are bonded to the lone pairs of the hydroxide ion's oxygen atom. The oxygen–ion–oxygen angle is 115.6° (O_a–O–O_b), substantially larger than the corresponding values for the F⁻(H₂O)₂ (91.4°) and H⁻(H₂O)₂ (77.4°) clusters. The large (O_a–O–O_b) angle results in an *R*(O_a–O_b) separation of 4.375 Å, which is 1.451 Å longer than in the water dimer.²³ It is evident that there is no hydrogen bond between the two water molecules, as indicated by the length of *R*(O_a–O_b) and the magnitude of the repulsive (+11.0 kcal/mol) water–water interaction at this geometry. The relative orientation of the two water molecules is determined by the much stronger hydroxide ion–water interaction. The relaxation of the two water molecules from the gas phase geometry is comparable, but less than in the *n* = 1 cluster. The

“free” OH stretches *R*(O_a–H_{2a}) and *R*(O_b–H_{2b}) continue to be unperturbed with respect to the water monomer.

For the *n* = 3 cluster we find two minima, also shown in Figure 1, which are qualitatively similar to the ones we reported earlier for the F⁻(H₂O)₃ cluster.²⁶ The first minimum has C₃ symmetry and resembles a “pyramidal” structure in which all water molecules act both as proton donors to the hydroxide ion and to another water as well as proton acceptors from another water. The basal interoxygen separation is 3.321 Å, longer by 0.521 Å than the corresponding separation in the water trimer²² but comparable (within 0.07 Å) to the one reported for the F⁻(H₂O)₃ cluster.²⁶ The weak hydrogen bond between the three water molecules is manifested by the small increase (0.002 Å) in the OH₂ involved in the hydrogen bond [*R*(O_χH_{2χ}), χ = a, b, c] with respect to water. In the water trimer these bonds are 0.011 Å longer²² than those found here.

The second minimum, denoted as “ring”, has C_s symmetry (the symmetry plane contains the atoms H, O, and O_b, cf. Figure 1). Only two water molecules are bonded to the hydroxide ion while the third one is bonded as a double donor to both of them. The path that interconverts these two minima is qualitatively similar to the one described for the F⁻(H₂O)₃ case.²⁶ By defining a common set of internal coordinates between the two minima, one can elucidate their interconversion pathway by linearly varying the internal coordinates from their initial (for the C₃ minimum) to their final set (for the C_s minimum). This path, commonly known as the Least Linear Motion (LLM) path, is shown in Figure 2. The isomerization mechanism between the C₃ and C_s minima is as follows: taking as reference the plane defined by the atoms (O, O_a, O_c), fragment (b) rotates counterclockwise with a simultaneous motion toward the reference plane. At the same time the (O_a–O–O_c) angle increase from 78.1° to 103.0°, two of the basal (O_cH_{2c}···O_b and O_aH_{2a}···O_c) as well as one of the ion–water (O_bH_{1b}···O) hydrogen bonds break, and a new one (O_bH_{1b}···O_c) is formed. Although there are two hydrogen bonds (a weaker water–water and a stronger ion–water) less in the C_s than in the C₃ minimum, the electronic energy of the former is only 1.15 kcal/mol less than the latter. The energetic penalty imposed by the loss of these two hydrogen bonds is partly compensated by the gain in the 2-body hydroxide–water interactions. Comparing the C_s with the C₃ minima, we note that *R*(O–O_a) is 0.08 Å shorter in the C_s than in the C₃ minimum and the strain associated with

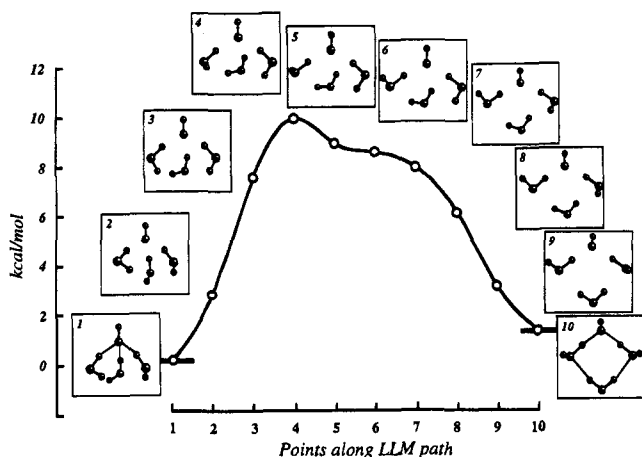


Figure 2. Least linear motion (LLM) path for the interconversion between the C_3 and C_s minima of the $\text{OH}^-(\text{H}_2\text{O})_3$ cluster.

the formation of the ring is removed, therefore resulting in stronger water–water interactions for the C_s minimum.

The intramolecular bends decrease with cluster size by 2.4° ($n = 1$), 2.1° , 2.3° ($n = 2$), and 1.5° , 2.4° ($n = 3$, ring) with respect to water. For the pyramidal isomer of the $n = 3$ cluster the relaxation is larger (4.1°) and comparable to the one in the $\text{F}^-(\text{H}_2\text{O})_3$ cluster²⁶ (3.9°) due to the strain associated with the formation of the ring and the simultaneous hydrogen bonding to the ion. In order to discuss the trends of the intramolecular OH bond lengths with cluster size, we classify them into the following four categories: (i) hydroxide ion bond length, (ii) water “free” OH distance, (iii) water “hydrogen bonded to hydroxide ion” OH distance, and (iv) water “hydrogen bonded to another water” OH distance.

The magnitude of type (i) bond distance decreases with cluster size, from 0.973 \AA (free OH^-) to 0.969 and 0.967 \AA for the $n = 1$ and 2 clusters, respectively. For the $n = 3$ cluster it is 0.964 (pyramidal) and 0.966 \AA (ring), almost identical to the “free” OH distance in water (cf. Table 1). The type (ii) bond distance is unperturbed with respect to water for the $n = 1, 2$ clusters and increases slightly (0.001 \AA) for the ring isomer of the $n = 3$ cluster (there is no “free” water OH distance for the pyramidal isomer). The variation of type (iii) is more dramatic: when compared to the “free” OH in water it is, for the $n = 1$ cluster, at least 0.124 \AA longer since it can practically move freely between the two oxygen atoms. Its relative elongation decreases to 0.068 and 0.073 \AA for the $n = 2$ cluster and to 0.079 \AA for the ring isomer of the $n = 3$ cluster. The latter exhibits a similar local environment around the ion as the $n = 2$ cluster by having two water molecules hydrogen bonded to OH^- . The $n = 3$ pyramidal isomer exhibits the least type (iii) relaxation (0.043 \AA), comparable to the one previously found for the $\text{F}^-(\text{H}_2\text{O})_3$ cluster.²⁶ Finally, the type (iv) bond distance is present only in the $n = 3$ cluster for which there exists hydrogen bonding between water molecules and is elongated by $+0.002$ (pyramidal) and $+0.014 \text{ \AA}$ (ring) with respect to water.

b. Harmonic Vibrational Frequencies. The harmonic vibrational frequencies for the $n = 1-3$ clusters together with the those for OH^- and H_2O are listed in Table 2. The numbers in square brackets denote the degeneracy of the mode due to symmetry (for the $n = 3$ isomers) while the numbers in parentheses identify the frequencies associated with the four types of OH stretches as classified in Section IIIa.

The calculated harmonic frequencies for water (at the MP2/aug-cc-pVDZ level) are 1623 , 3805 , and 3940 cm^{-1} , all within 25 cm^{-1} of the experimental²⁹ values of 1648 , 3832 , and 3943

Table 2. Harmonic Vibrational Frequencies (in cm^{-1}) for OH^- , H_2O , and $\text{OH}^-(\text{H}_2\text{O})_n$ ($n = 1-3$)^a

OH^-	H_2O	$\text{OH}^-(\text{H}_2\text{O})$	$\text{OH}^-(\text{H}_2\text{O})_2$	$\text{OH}^-(\text{H}_2\text{O})_3$	
				pyramidal	ring
3767 (i)	1623	207	18	42 [2]	50
	3805 (ii)	328	99	45	77
	3940 (ii)	453	161	241 [2]	145
		570	283	298 [2]	194
		1321	306	329 [2]	214
		1608 (iii) ^b	345	348	228
		1729 (iii) ^b	454	469	307
		3814 (i)	542	529	339
		3864 (ii)	575	538 [2]	351
			1138	970	428
			1163	980 [2]	544
			1690	1712 [2]	571
			1703	1717	612
			2453 (iii)	3029 [2] (iii)	695
			2642 (iii)	3177 (iii)	769
			3834 (i)	3829 (iv)	1161
			3876 (ii)	3832 [2] (iv)	1209
			3878 (ii)	3870 (i)	1693 [2]
					1721
					2293 (iii)
					2506 (iii)
					3579 (iv)
					3649 (iv)
					3845 (i)
					3873 [2] (ii)

^a Numbers in square brackets denote degeneracy while parentheses identify frequencies associated with the four types of OH stretches, defined in Section IIIa. Frequencies corresponding to the modes with the largest IR intensities of Figure 3 are indicated in boldface. ^b Type (iii) OH stretch coupled with intramolecular bend.

cm^{-1} . Accordingly, the computed harmonic frequency for OH^- is within 70 cm^{-1} of the experimental³⁰ estimate of 3700 cm^{-1} .

In agreement with the trends of the intramolecular bends with cluster size discussed in Section IIIa, we note that the frequency associated with the intramolecular bending mode is blue-shifted with respect to the corresponding frequency in water upon clustering. For $n = 1$ it is coupled with the hydrogen-bonded (O_a-H_{1a}) stretch (1608 and 1739 cm^{-1}). For $n = 2$ it increases by 67 and 80 cm^{-1} with respect to water. It continues to increase for $n = 3$ by 89 and 94 cm^{-1} for the pyramidal and 70 and 98 cm^{-1} for the ring isomers, respectively. These shifts are larger than those previously reported for the ring water clusters²³ but comparable in magnitude with the corresponding values for the $\text{F}^-(\text{H}_2\text{O})_3$ clusters.²⁶

As regards the frequencies associated with the four types of OH stretches (i)–(iv), defined in Section IIIa, the type (i) frequency increases by 47 ($n = 1$), 67 ($n = 2$), 103 ($n = 3$, pyramidal), and 78 cm^{-1} ($n = 3$, ring) with respect to OH^- (3767 cm^{-1}). For the pyramidal isomer of the $n = 3$ cluster it is 3870 cm^{-1} , almost identical with the average of the frequencies corresponding to the symmetric and asymmetric stretches in water (3873 cm^{-1}) therefore scrambling with the frequencies of the “free” [type (ii)] OH stretches. This is due to the fact that the bond length of the hydroxide ion decreases with cluster size, effectively becoming a “free” [type (ii)] OH stretch for $n = 3$ (cf. Table 1). The frequency for type (ii) “free” OH stretch remains almost unchanged (within $\pm 10 \text{ cm}^{-1}$) from the average of the symmetric and asymmetric stretches in water (3873 cm^{-1}), a corollary of the fact that the corresponding “free” OH stretch in clusters $n = 1-3$ changes by

(29) Benedict, W. S.; Gailar, N.; Plyer, E. K. *J. Chem. Phys.* **1956**, *24*, 1139.

(30) Huber, K. P.; Herzberg, G. *Molecular Spectra and Molecular Structure. IV. Constants of Diatomic Molecules*; van Nostrand Reinhold Co.: New York, 1979; p 516.

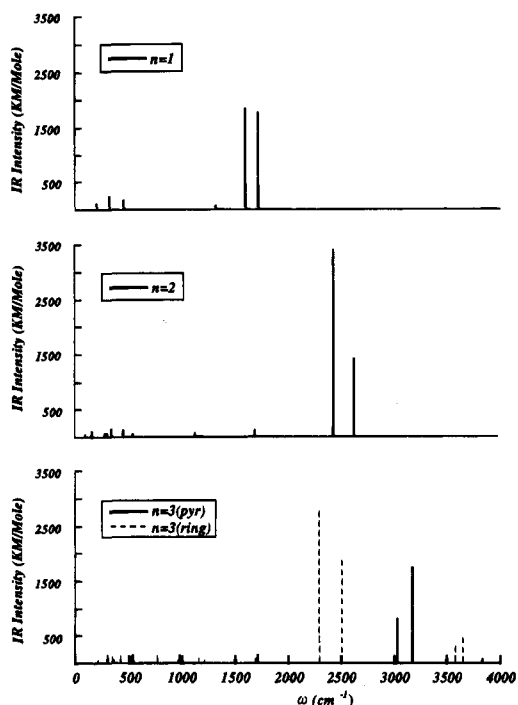


Figure 3. Infrared (IR) intensities (in KM/mol) for the $\text{OH}^-(\text{H}_2\text{O})_n$ ($n = 1-3$) clusters. For the $n = 3$ cluster the dashed lines correspond to the ring isomer.

$\leq 0.001 \text{ \AA}$ from the OH stretch in water. Type (iii) frequencies exhibit the largest shift with respect to the *average* of the symmetric and asymmetric stretches in water, a consequence of the large decrease in the type (iii) bond length change with cluster size. For $n = 1$, the type (iii) harmonic frequency is shifted by 2144 cm^{-1} to the red, 540 cm^{-1} more than the one seen for the $\text{F}^-(\text{H}_2\text{O})$ cluster.²⁶ Since the $n = 1$ cluster is not rigid this red shift can be considered as a lower limit. The red shift of the type (iii) harmonic frequency is $1231, 1420 \text{ cm}^{-1}$ for the $n = 2$ cluster and $1367, 1580 \text{ cm}^{-1}$ for the ring isomer of the $n = 3$ cluster. The analogous shift to the red with respect to water (3873 cm^{-1}) is smaller but substantial (696 and 844 cm^{-1}) for the pyramidal isomer of the $n = 3$ cluster. Finally, the type (iv) frequencies are found only in the two isomers of the $n = 3$ cluster for which there exists hydrogen bonding between water molecules. For the pyramidal isomer the elongation of the hydrogen bonded to water OH stretch is only 0.002 \AA and the corresponding frequencies are red-shifted by only 41 and 44 cm^{-1} with respect to the *average* of the symmetric and asymmetric stretches in water (3873 cm^{-1}). The relaxation is, however, larger (0.014 \AA) for the double acceptor fragment (labeled "b" in Figure 1) of the ring isomer resulting in a larger shift of 224 and 294 cm^{-1} to the red with respect to water. The latter is comparable to the corresponding red shift previously seen for the water trimer^{22,23} which exhibits similar relaxation (0.013 \AA) of the hydrogen-bonded OH stretches.

The frequencies corresponding to the modes with the largest IR intensities are indicated in boldface in Table 2, and their intensities are shown in Figure 3. The most active IR modes are the ones associated with type (iii) frequencies (OH stretches hydrogen bonded to the hydroxide ion) as they exhibit the largest dipole moment change. The displacements of the atoms along the normal modes with the most active IR frequencies are shown in Figure 4 in which the harmonic frequency (in cm^{-1}) and IR intensity (in KM/mol) of each mode are also indicated. The modes are numbered by magnitude in ascending order (cf. Table 2). For $n = 1$ the two most active IR modes, having comparable intensities, correspond to a coupling of the water bend with the

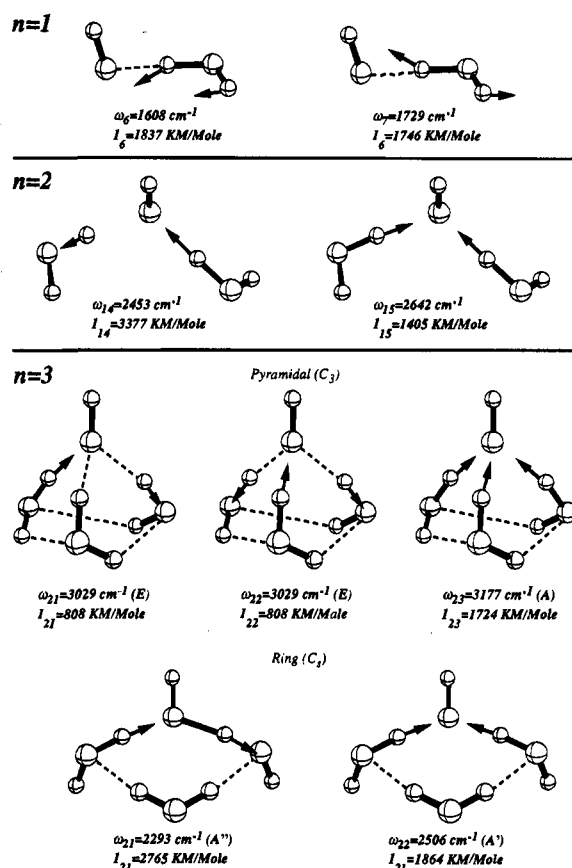
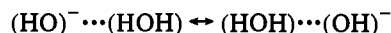
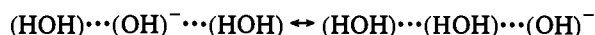


Figure 4. Displacements of the atoms along the modes with the largest IR intensities of Figure 3 for $n = 1-3$. The harmonic frequency and IR intensity of each mode are also indicated. Modes are numbered by magnitude in ascending order (cf. Table 2).

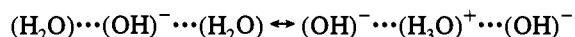
hydrogen-bonded OH stretch. Along these two modes the largest motion occurs for the hydrogen-bonded proton resulting in a charge transfer from the one to the other side of the molecule to accommodate the isomerization



For $n = 2$ the most IR active mode with frequency 2453 cm^{-1} is associated with the out-of-phase motion of the hydrogen-bonded protons representing



This is occurring via a single proton transfer from the water to the hydroxide ion, as in the $n = 1$ case. A second mode of less intensity at 2453 cm^{-1} corresponds to the in-phase motion of the two hydrogen bonded protons toward the oxygen atom of the hydroxide ion, i.e.,

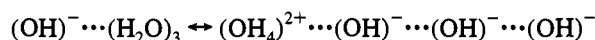


which occurs via two proton transfers. A similar trend is observed for the ring isomer of the $n = 3$ cluster which has the same local environment (two water molecules) around the hydroxide ion. The mode with the largest IR intensity (2293 cm^{-1}) corresponds to the out-of-phase motion of the hydrogen-bonded protons while their in-phase motion (2506 cm^{-1}) is associated with a less IR active mode as in the $n = 2$ case. The double donor water molecule simply acts as a spectator, shifting the magnitudes of these two frequencies by $\sim 150 \text{ cm}^{-1}$ to the red with respect to the $n = 2$ case.

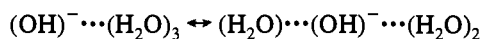
Table 3. Electronic (E_e) and Zero-Point (E_0) Energies for OH^- , H_2O , and $\text{OH}^-(\text{H}_2\text{O})_n$ ($n = 1-3$) at the MP2 Level

species	basis set	E_e (au)	E_0 (kcal/mol)
OH^-	aug-cc-pVDZ	-75.639 281	5.38
	aug-cc-pVTZ	-75.716 003	
H_2O	aug-cc-pVDZ	-76.263 385	13.39
	aug-cc-pVTZ	-76.344 148	
$\text{OH}^-(\text{H}_2\text{O})$	aug-cc-pVDZ	-151.945 438	19.86
	aug-cc-pVTZ	-152.104 202	
$\text{OH}^-(\text{H}_2\text{O})_2$	aug-cc-pVDZ	-228.244 097	35.97
	aug-cc-pVTZ	-228.244 097	
$\text{OH}^-(\text{H}_2\text{O})_3$ pyramidal (C_3) ring (C_2)	aug-cc-pVDZ	-304.538 538	52.84
	aug-cc-pVDZ	-304.536 714	52.35

In contrast, for the pyramidal isomer of the $n = 3$ cluster, the mode at 3177 cm^{-1} associated with the three proton transfer process



is more active than the two degenerate ones at 3029 cm^{-1} corresponding to a single proton transfer from one of the water molecules to the hydroxide ion



c. Energetics. The MP2 electronic (E_e) and zero-point (E_0) energies for the optimal structures of the clusters as well as OH^- and H_2O are shown in Table 3 with the aug-cc-pVDZ ($n = 1-3$) and aug-cc-pVTZ ($n = 1$) basis sets. The incremental association energies are listed in Table 4. Numbers in parentheses correspond to the results with the aug-cc-pVTZ basis set. $(\Delta E_e)_{n,n-1}$ denotes electronic energy differences whereas $(\Delta E_0)_{n,n-1}$ includes zero-point harmonic vibrational energy conditions. Our MP2/aug-cc-pVDZ ΔE_e for the $n = 1$ cluster is within 0.3 kcal/mol of the one reported by Szczesniak and Scheiner¹⁴ at the MP3 level of theory with the 6-311G** basis set augmented with a set of very diffuse p functions on oxygen. Our results support the finding by Szczesniak and Scheiner¹⁴ regarding the importance of diffuse functions in the basis set and the significance of electron correlation. The latter is also apparent from the large overestimation of the binding at the HF level of theory during earlier^{13,14,16} studies. The use of a larger (aug-cc-pVTZ) basis set increases ΔE_e by 0.8 kcal/mol at the MP2 level of theory. This trend is qualitatively similar to the one found for the $\text{F}^-(\text{H}_2\text{O})$ cluster²⁶ for which, however, inclusion of higher correlation at the MP4 level had the opposite effect of reducing the binding energy. A more systematic investigation of the basis set and electron correlation effect on the binding energy will be presented in a future study of the $n = 1$ PES.

The binding energies of Table 4 for the $n = 2, 3$ clusters are, to our knowledge, the first ones reported at the correlated level. Our previous study of the $\text{F}^-(\text{H}_2\text{O})_n$ clusters suggested that the use of HF geometries to perform correlated calculations introduces significant errors due to the large geometry relaxation upon inclusion of electron correlation. In particular, previous HF calculations^{16,17} overestimated the incremental binding

Table 4. Incremental Association Electronic Energies, $(\Delta E_e)_{n,n-1}$, and Enthalpies, $(\Delta H^{298\text{K}})_{n,n-1}$, at 298 K^a

n	$(\Delta E_e)_{n,n-1}$	$(\Delta E_0)_{n,n-1}$	$(\Delta H^{298\text{K}})_{n,n-1}$	exp			
1	-26.8 (-27.6)	-25.8 (-26.6)	-27.0 (-27.8)	-34.6 ^b	-22.5 ^c	-25.0 ^d	-26.5 ± 1.0 ^e
2	-22.1	-19.4	-20.1	-23.1 ^b	-16.4 ^c	-17.9 ^d	-17.6 ± 1.0 ^e
3 pyramidal	-19.5	-16.0	-16.9	-18.4 ^b	-15.1 ^c		-16.2 ± 1.0 ^e
	-18.3	-15.4	-16.5				

^a $(\Delta E_0)_{n,n-1}$ includes zero-point energy vibrational corrections. All results are at the MP2 level. Numbers in parentheses correspond to the results with the aug-cc-pVTZ basis set. Units are kcal/mol. ^b Reference 9. ^c Reference 10. ^d Reference 11. ^e Reference 12.

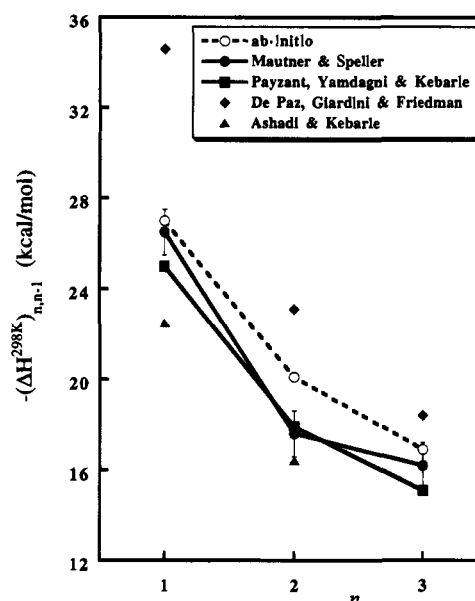


Figure 5. Variation of the incremental association enthalpies $(\Delta H^{298\text{K}})_{n,n-1}$ with cluster size. Filled symbols, solid lines correspond to experimental and open symbols, dashed line to the *ab initio* results. Error bars of ± 1 kcal/mol in the experimental measurements of Mautner and Speller are also indicated.

energies of the $n = 2, 3$ clusters by as much as 50% with respect to experiment and our MP2 results. We finally note that inclusion of zero-point energy corrections decreases the energy difference between the pyramidal and ring isomers of the $n = 3$ cluster to ~ 0.6 kcal/mol.

In order to compare our results with experiment, we have estimated the incremental enthalpies of formation at 298 K, $(\Delta H^{298\text{K}})_{n,n-1}$, using classical corrections^{26,27} for the changes in vibrational, rotational, and translational energies from 0 to 298 K as well as the ΔPV term. They are shown, together with the previous experimental estimates, in Table 4. Our MP2/aug-cc-pVDZ incremental association enthalpies together with the previous experimental results⁹⁻¹² for $n = 1-3$ are shown in Figure 5. Open symbols denote the *ab initio* whereas filled symbols correspond to the experimental results. The solid lines trace the two most recent sets of experimental measurements by Mautner and Speller¹² (MS) and Payzant, Yamdagni, and Kebarle¹¹ (PYK) and the dashed line traces the *ab initio* results. MS are the only ones who assign error bars of ± 1.0 kcal/mol in their measurements on the basis of the standard deviation of the slopes of van't Hoff plots and the precision of replicate measurements between several laboratories. Our results are within the error bars of those by MS for $n = 1$ and 3 but overestimate the $n = 2$ case by ~ 2.0 kcal/mol. Our $(\Delta H^{298\text{K}})_{1,0}$ is within 0.6 kcal/mol of the value reported by Del Bene²⁰ at the MP4/6-31+G(2d,2p) level of theory. The overall variation of the incremental enthalpies of formation with n is similar between the *ab initio* and the results of PYK, the latter systematically yielding enthalpies lower by 2.0 kcal/mol (cf. Figure 5 and Table 4). In contrast, the measurements of MS

Table 5. Energy Decomposition for the C_3 and C_s Isomers of the $n = 3$ Cluster at the MP2/aug-cc-pVDZ Level^a

terms				OH ⁻ (H ₂ O) ₃	
i	j	k	l	pyramidal (C ₃)	ring (C _s)
I	w _a			-25.8	-29.4
I	w _b			-25.8	-11.8
I	w _c			-25.8	-29.4
w _a	w _b			-0.5	-3.6
w _a	w _c			-0.5	1.5
w _b	w _c			-0.5	-3.6
I	w _a	w _b		2.6	-1.5
I	w _a	w _c		2.6	3.8
I	w _b	w _c		2.6	-1.5
w _a	w _b	w _c		-0.4	1.2
I	w _a	w _b	w _c	-0.1	0.7
	relaxation			3.2	6.4
	total 2-body			-78.9	-76.3
	total 3-body			7.4	2.0
	4-body			-0.1	0.7
	interaction energy			-68.4	-67.2

^a The hydroxide ion is denoted by I whereas the three water molecules are denoted by w_j (j = a, b, c) respectively as shown in Figure 1.

show a “dip” at $n = 2$. Would the variation of the MS results have been the same as those by PYK, their result for $n = 2$ would have agreed with our estimate. It should be noted that MS used D₂O in their experiments, but found no measurable difference between the clustering thermochemistry in light and heavy water systems within their error bar of ± 1 kcal/mol and ± 2 cal/(mol K). Sources of error in our estimates of $(\Delta H^{298K})_{n,n-1}$ are associated with inaccuracies in the various pieces that contribute to the enthalpy. These include the calculation of electronic energy changes at the MP2/aug-cc-pVDZ level of theory, the employment of classical corrections for the temperature dependence of the translational and rotational energies, and the use of harmonic vibrational frequencies to account for the magnitude and temperature dependence of the vibrational energy.

It is finally of interest to investigate the origin of the electronic energy difference (1.2 kcal/mol) between the two isomers of the $n = 3$ cluster. The energy of each cluster was decomposed in terms of 2-, 3-, and 4-body interactions (where “body” denotes either a water molecule or the hydroxide ion) in a manner similar to the one used in earlier studies of water²⁴ and fluoride–water²⁶ clusters. The results are shown in Table 5 in which the hydroxide ion is denoted by “I” and the three water molecules as w_a, w_b, and w_c respectively, in a manner consistent with the labeling of the fragments in Figure 1.

We first note that the relaxation energy of the fragments (cluster vs gas phase geometries) is larger by 3.2 kcal/mol in the ring than in the pyramidal isomer. It mainly arises from the relaxation of the water fragments w_a and w_c in which the bond lengths $R(\text{O}_a-\text{H}_{1a})$ and $R(\text{O}_c-\text{H}_{1c})$ are 0.036 Å longer in the ring than in the pyramidal isomer respectively (cf. Table 1). Since the energy of fragments w_a and w_c (at the cluster geometry) is raised due to their relaxation, so is the asymptote with respect to which the interactions (I–w_a) and (I–w_c) are computed. These are -29.4 kcal/mol for the ring isomer, 2.6 kcal/mol larger than the corresponding ion–water interaction in the $n = 1$ cluster (cf. Table 4). The interaction (I–w_b) is attractive but weaker (-11.8 kcal/mol) due to the large distance and orientation of fragment w_c with respect to hydroxide ion in the ring isomer. In contrast, all ion–water interactions are -25.8 kcal/mol in the pyramidal isomer.

As regards the water–water 2-body interactions, they are all -0.5 kcal/mol in the pyramidal isomer, much weaker than the corresponding values in the water trimer²⁴ (-4.64 to -5.04 kcal/

mol) but comparable to that in the pyramidal isomer of the F⁻(H₂O)₃ cluster²⁶ (-0.25 kcal/mol). This result is consistent with the fact that the oxygen–oxygen separation in the pyramidal isomer is 0.52 Å longer than the corresponding one in the water trimer.^{22,23} For the ring isomer, there are two strong (-3.6 kcal/mol) donor–acceptor interactions [(w_a-w_b) and (w_b-w_c)] whereas the (w_a-w_c) interaction is repulsive (+1.5 kcal/mol). The total 2-body interaction sums up to -78.9 and -76.3 kcal/mol for the pyramidal and ring isomers, respectively.

The different hydrogen bonding network found in the two isomers gives rise to dissimilar 3-body interactions. For the pyramidal isomer, all ion–water–water 3-body interactions are repulsive (2.6 kcal/mol). For the ring isomer, the interaction (I–w_a-w_c) which is qualitatively similar to the one found in the pyramidal isomer (both water molecules bonded to hydroxide ion) is also repulsive (3.8 kcal/mol). In contrast, (I–w_a-w_b) and (I–w_b-w_c) correspond to a configuration in which the second water molecule is bonded to the first water resulting in an attractive (-1.5 kcal/mol) interaction. The water hydrogen bonding network in the pyramidal isomer resembles the corresponding one found in the water trimer, i.e., all water molecules act as proton donors and proton acceptors. The interaction is, however, smaller (-0.41 kcal/mol) in the pyramidal isomer than in the water trimer²⁴ (-2.27 kcal/mol). This is due, again, to the fact that the three water molecules are more loosely bound to each other in the former than in the latter case. In contrast, the hydrogen bonding network in the ring isomer is of a different kind (acceptor–double donor–acceptor) resulting in a repulsive 3-body interaction of 1.2 kcal/mol. The total 3-body interaction is therefore repulsive for both isomers (7.0 kcal/mol for the pyramidal and 2.0 kcal/mol for the ring isomers, respectively). Finally, the 4-body term is negligible (-0.1 kcal/mol) for the pyramidal but a bit stronger and repulsive (0.7 kcal/mol) for the ring isomer.

IV. Conclusions

In this study we have reported the geometries, harmonic vibrational frequencies, and incremental association enthalpies for the OH⁻(H₂O)_n ($n = 1-3$) clusters. Clusters with $n = 2$ and 3 are the first ones reported at the correlated level. In agreement with previous calculations for the $n = 1$ cluster^{14,20} we have found that both electron correlation and diffuse functions in the orbital basis set are necessary in order to produce accurate binding energies. The interaction between the hydroxide ion and water is very strong, comparable to the corresponding one for F⁻. The structure of the $n = 1$ cluster is non-rigid due to the barrierless isomerization that occurs via the motion of the hydrogen-bonded proton between the two oxygen atoms. For the $n = 2$ cluster, there is no hydrogen bonding between the two water molecules, their orientation is determined by their much stronger interaction with OH⁻. As the cluster grows, the water–water interaction becomes more important as is evident from the corresponding decrease in the O–O separations. For the $n = 3$ cluster, we have found two isomers having electronic energy differences within 1.2 kcal/mol and enthalpies of formation within 0.4 kcal/mol. Hydrogen bonding between water molecules is stronger in the ring than in the pyramidal isomer as can be deduced from the larger relaxation of type (iv) OH stretches (Table 1) and the red shifts in the corresponding frequencies (Table 2). This is also manifested by the magnitudes of the 2- and 3-body interaction terms between water molecules in the two isomers. The two isomers of the $n = 3$ cluster exhibit a different hydrogen bonding network, a fact that is reflected in the different signs and magnitudes of the corresponding 3-body water interaction energy

terms (cf. Table 5). The existence of the ring isomer and the fact that it is almost isoenergetic and exhibits a stronger water-water hydrogen bonding than the pyramidal one can explain the experimental observation by van Doren *et al.*,⁷ namely that $\text{OH}^-(\text{H}_2\text{O})$ and $(\text{H}_2\text{O})_2$ were generated almost exclusively from $\text{OH}^-(\text{H}_2\text{O})_3$ following collisional dissociation in a reaction flow tube. This can occur via a simultaneous cleavage of the stronger ($\text{O}-\text{H}_{1a}$) and the weaker (O_c-H_{1b}) hydrogen bonds and can be assisted by the low-barrier proton transfer of the hydrogen-bonded protons H_{1a} and H_{1c} (cf. Figure 1).

Hydration decreases the bond length of OH^- ; by the time the third water is added it has the same value as the "free" OH in water resulting in "scrambling" of its frequency. Furthermore, only the type (iii) OH stretches (OH's hydrogen bonded to the hydroxide ion) were found to be strongly IR active. These results are consistent with experimental observations³ that found that the hydroxide stretch ($\sim 3600\text{ cm}^{-1}$) is very weak in the IR and a very strong band exists from 2500 to 3000 cm^{-1} . From Table 2 it is evident that this band corresponds to the water OH stretches that are hydrogen bonded to the hydroxide ion [type (iii), indicated in boldface in Table 2]. For $n = 2$ the corresponding frequencies are 2453 and 2642 cm^{-1} , while they cover the range 2293– 3177 cm^{-1} for the two isomers of the $n = 3$ cluster. Finally, the relatively strong polarized peak at $\sim 290\text{ cm}^{-1}$ in the low-frequency range of the Raman spectra, which has been assigned to the symmetric hydrogen-bonded stretching vibration of the $\text{OH}^-(\text{H}_2\text{O})$ cluster, is consistent with our result of 328 cm^{-1} for the same mode (Table 2). The range

of the harmonic frequency of this mode remains very narrow with cluster size: it is 345 cm^{-1} for $n = 2$ and 348, 339 cm^{-1} for the pyramidal and ring isomers of the $n = 3$ cluster.

Note Added in Proof: An independent study by A. R. Grimm, G. B. Bacskay, and A. D. J. Haymet (*Mol. Phys.*, in press) has recently been carried out, focusing on the computation of the free energy of solvation of OH^- via the self-consistent reaction field method. These authors estimated the effect of the first hydration shell ($n = 3$) from gas phase cluster calculations. They reported geometries and energies of the $n = 1-4$ clusters at the MP2 level of theory with the DZP(s,p) basis set. Although our results agree for the $n = 1$ and 2 clusters, they are qualitatively different for the $n = 3$ cluster for which Grimm, Bacskay, and Haymet do not report the ring structure but another one having a rather extended geometry.

Acknowledgment. We thank Dr. T. H. Dunning, Jr., for many helpful discussions and continuous support. This work was performed under the auspices of the Office of Basic Energy Sciences, Division of Chemical Sciences, U.S. Department of Energy, under contract No. DE-AC06-76RLO 1830. Computer resource allocations at the National Energy Research Super-computer Center (Livermore, CA) were provided by the Scientific Computing Staff, Office of Energy Research, U.S. Department of Energy.

JA951446W